specificity (i.e., binding of the probe to a perfectly matched sequence rather than to regions with sequence mismatches).

Seven primer/probe sets were designed for this study. Fig. 1 shows a schematic diagram of the strategy for mutation detection using these primer/probe sets. Tables 1 and 2 list the primer/probe sets and corresponding sequences and primer concentrations that were used to target the 11 mutations. Primer/probe sets A, B, C, D, E, and F were designed to detect mutations [I], [II], [III], [IV], [V], and [XIX], respectively. Primer/probe set G was designed to detect the five mutations clustered on exon 17: mutations [VI], [VII], [VIII], [IX], and [XXI] (Fig. 1D). All primers and probes were synthesized based on the NCBI reference SLC25A13 gene sequence (GenBank accession no. **NM_014251**) with the exception of mutation [XIX]:IVS16ins3kb, which was designed according to [19].

Real-time PCR and subsequent melting curve analyses were performed in a closed tube using a 20-μL mixture on a LightCycler 1.5 (Roche Diagnostics, Tokyo, Japan). The PCR mixture contained 2.0 μL of genomic DNA (10–50 ng), 0.5 μM of forward primer, 0.5 or 0.1 μM of reverse primer, 0.2 μM of each sensor and anchor probe, and 10 μL of Premix ExTaq™ (Perfect Real Time) reagent (TaKaRa Bio Inc., Otsu, Japan).

The thermal profile conditions were identical for all seven assays and consisted of an initial denaturation step (30 s at 95 °C), followed by 45 amplification cycles with the following conditions: denaturation for 5 s at 95 °C and annealing and extension for 20 s at 60 °C. The transition rate between all steps was 20 °C/s. After amplification, the samples were held at 37 °C for 1 min, followed by the melting curve acquisition at a ramp rate of 0.15 °C/s extending to 80 °C with continuous fluorescence acquisition.

Table 2
Primers, probes and target amplicon sequences, target mutation sites, and primer concentrations.

Primer/probe set	Name	Sequences of PCR products, primer locations, probe sequences, and mutation sites (5′ to 3′)	Concentration (μmol/L)
A		GGCTATACTGAAATATGAGAAatgaaaaagggatgtttttaaatttataatgtaaattgtaataaattggtatatttgttgcttgtgtttgtttttcccctacagac	
		gtatgaccttagcagacattgaacggattgctcctctggaagagggaactctgccCTTTAACTTGGCTGAGG (181 bp)	
	Mut1-F	GGCTATACTGAAATATGAGAA	0.5
	Mut1-R	CCTCAGCCAAGTTAAAG	0.5
	Mut1-UP	ATGTAAATTGTAATAAATTGGTATATTTGTTGCTTGTGTT-FITC	
	Mut1-DW	LC Red640-GTTTTTCCCCTACAGAC**GACC**-P	
B		GAATGCAGAACCAACGAtcaactggctcttttgtgggagaactcatgtataaaaacagctttgactgttttaagaaagtgctacgctatgaaggcttctt	
		tggactgtatagaggttagtgccacatgctcaatacctgttaggtgaaataacactcaaaggtttggtttctcatcttagtgcctGACATGAATTAGCAAGACTG (205 bp)	
	Mut2-F	GAATGCAGAACCAACGA	0.5
	Mut2-R	CAGTCTTGCTAATTCATGTC	0.1
	Mut2-UP	ACCTAACAGGTATTGAGCATGTG-FITC	
	MUt2-DW	LC Red640-CACTAA**C**CTCTATACAGTCCA-P	
C		GCAGTTCAAAGCACAGTTATTtttatatagtgagaatgtgaccagactgagatggtgttgtgtctctcctgcaggtatgcctgcagcatctttagtg	
		accccctgctgatgttatcaagacgagattacaggtg	
		gctgcccggg(**gagatta**caggtggctgcccggg)ctggccaaaccaCTTACAGCGGAGTGATAGAC (175 bp)	
	Mut3-F	GCAGTTCAAAGCACAGTTATT	0.5
	Mut3-R	GTCTATCACTCCGCTGTAAG	0.5
	Mut3-UP	ACCCCTGCTGATGTTATCAAGACGAGATTACAGGT-FITC	
	Mut3-DW	LC Red640-GCTGCCCGGG**GAGATTA**-P	
D		TCAATTTATTTGAGGCTGCtggaggtaccacatcccatcaagttagtttctcctattttaatggatttaattcgctccttaacaac	
		atggaactcattagaaagatctatagcactc	
		tggctggcaccaggaaagatgttgaagtGACTAAGGGTGAGTGAGAA (164 bp)	
	Mut4-F	TCAATTTATTTGAGGCTGC	0.5
	Mut4-R	TTCTCACTCACCCTTAGTC	0.5
	Mut4-UP	AATGGATTTAATT**C**GCTCCTTAACA-FITC	
	Mut4-DW	LC Red640-ATGGAACTCATTAGAAAGATCTATAGCACTC-P	
E		TGCACAAAGATGGTTCGgtcccacttgcagcagaaattcttgctggaggctgc**g**taagtacctttgaagctctcttcattgaaaagacttgtttcac	
		atatatatcactaccatggtcaacaggtgtggactaaggcttctgttTAACCACAGATCCTGCA (162 bp)	
	Mut5-F	TGCACAAAGATGGTTCG	0.5
	Mut5-R	TGCAGGATCTGTGGTTA	0.5
	Mut5-UP	GTGAAACAAGTCTTTTCAATGAAGAGAGCTTC-FITC	
	Mut5-DW	LC Red640-AAGGTACTTA**C**GCAGCCTC-P	
F	normal allele	GGAGCTGGTGGTATGGAAatagtgtgttcttaactaactctttggtatcaggtaaatttttaaaatatctaattatatctgtgatttctc	
		catttttttaaagctcgtgtatttcgatcctcaccccagtttggt	
		gtaactttgctgacttacgaattgctacagcgatggttctacattgattttggaggagtgtaagtatcatgctaaatctgctgctaaatttt	
		GGCTGCTGCTAATGCTC (244 bp)	
	insertion allele	CCATCTTCCTCCTCCCTTggcagccccgccccccgatttctccatttttttaaagctcgtgtatttcgatcctcaccccagtttggt	
		gtaactttgctgacttacgaattgctacagcgatggttctacattgatttt	
		ggaggagtgtaagtatcatgctaaatctgctgctaaattttGGCTGCTGCTAATGCTC (196 bp)	
	Mut19-N-F	GGAGCTGGTGGTATGGAA	0.5
	Mut19-ins-F	CCATCTTCCTCCTCCCTT	0.5
	Mut19-R	GAGCATTAGCAGCAGCC	0.5
	Mut19-UP	ACCAAACTGGGGTGAGGATCGAAATACACGAGCTTTAAAAAAATG-FITC	
	Mut19-N-DW	LC Red640-AGAAATCACAGATATAATTAGATATTT-P	
	Mut19-ins-DW	LC Red640-AGAAATCGGGGGGCGGGG-P	
G		TCTTAACTAACTCTTTGGTATCAGGTaaatttttaaaatatctaattatatctgtgatttctccatttttttaaagctcg	
		tgtatttcgatcctcaccccagtttggtgtaactttgc**t**gactt**a(a)cg**aattgctacag**c**ga	
		tggttctacattgattttggaggagtgtaagtatcatgctaaatctgctgctaaattttGGCTGCTGCTAATGCTC (217 bp)	
	Mut6-9, 21-F	TCTTAACTAACTCTTTGGTATCAGGT	0.5
	Mut6-9, 21-R	GAGCATTAGCAGCAGCC	0.5
	Mut6-9, 21-UP	TGTATTTCGATCCTCACCCCAGTTTGGTGTAACTT-FITC	
	Mut6-9, 21-DW	LC Red640-GC**G**GACTT**ACG**AATTGCTACAG**C**GA-P	

Upper case and underlined letters indicate the locations of primers and probes, respectively. Inserted DNA is shown in parenthesis. Nucleotides in boldface were used for mutation detection.
F: forward, R: reverse, UP: upstream, DW: downstream, N: normal allele, ins: insertion allele, FITC: fluorescein isothiocyanate, P: phosphate.

Please cite this article as: A. Kikuchi, et al., Simple and rapid genetic testing for citrin deficiency by screening 11 prevalent mutations in *SLC25A13*, Mol. Genet. Metab. (2012), doi:10.1016/j.ymgme.2011.12.024

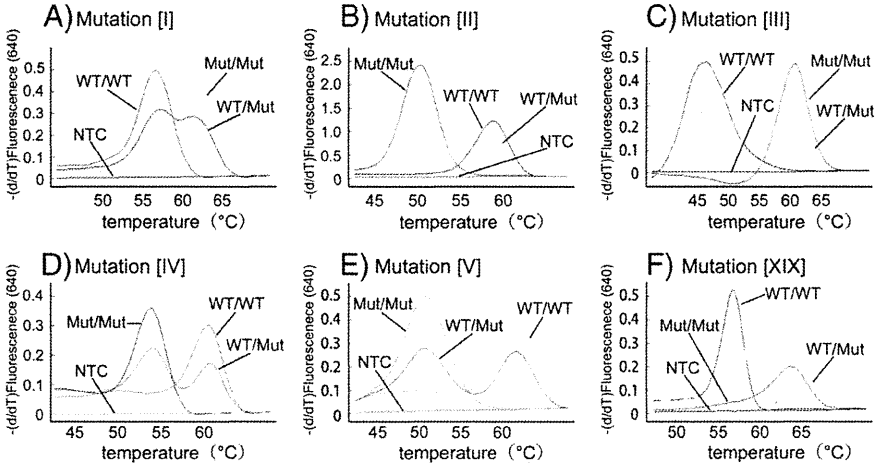

Fig. 2. Typical melting curves used in the detection of mutations [I–V] and [XIX]. Each assay using primer/probe sets A–F is displayed in a separate graph (A–F). WT: wild-type allele, Mut: mutant allele, NTC: no DNA template control.

2.3. Validation of the mutation detection system

After establishing the protocol for detecting the 11 prevalent mutations, 50 DNA samples from patients' blood were sent from Kagoshima University to Tohoku University for the validation of this system in a single-blind manner. Similarly, 26 DNA samples purified from paper-filter blood samples were analyzed in the same manner as the blood DNA samples.

2.4. Estimation of the carrier frequency

For the estimation of the heterozygous carrier frequency, 420 genomic DNA samples from healthy volunteers were screened using the HybProbe analysis for the 11 prevalent mutations. All detected mutations were confirmed by direct sequencing.

2.5. Ethics

This study was approved by the Ethical Committees of Tohoku University School of Medicine and Kagoshima University. Written informed consent was obtained from all participants or their guardians.

3. Results

3.1. Development of the mutation detection system

In primer/probe sets B, D, and E, the reporter probes were designed to be complimentary to the wild-type allele (Fig. 1A). To allow for an improved detection of the mutations, primer/probe sets A and C were designed to be complementary to the mutant allele (Figs. 1B, C). In the primer/probe set F, two forward PCR primers, which were specific to the wild-type and the mutant alleles, were used with a common reverse primer for the co-amplification of the wild-type and 3-kb insertion alleles (Fig. 1E). Two reporter probes, which had a common anchor probe, were used for the detection of the wild-type and mutant alleles. Because the two reporter probes had different melting temperatures, we were able to identify the allele that was amplified. Fig. 2 shows representative results of the melting curve analyses using the primer/probe sets A–F, in which all of the mutant alleles generated distinct peaks corresponding to the wild-type alleles.

In the primer/probe set G, we used a reporter probe that was complementary to the mutant [XXI] allele (Fig. 1D). All five mutations in exon 17 were successfully differentiated from the wild-type allele (Figs. 3A–E). The [XXIX] mutation is an additional mutation in exon

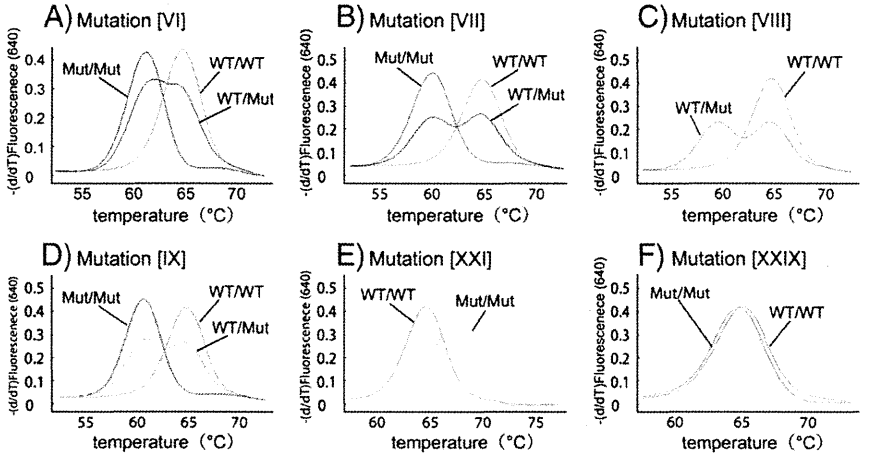

Fig. 3. Typical melting curves used in the detection of mutations [VI–XI], [XXI], and [XXIX] on exon 17. Genotyping was performed using primer/probe set G. Each melting curve for a target mutation is displayed in a separate graph (A–F). Note that mutation [XXIX] (F) is a non-target mutation on the anchor probe. WT: wild-type allele, Mut: mutant allele.

Please cite this article as: A. Kikuchi, et al., Simple and rapid genetic testing for citrin deficiency by screening 11 prevalent mutations in *SLC25A13*, Mol. Genet. Metab. (2012), doi:10.1016/j.ymgme.2011.12.024

17 that is not listed in Table 1. The [XXIX] mutation is located in the anchor-probe binding site and not on the reporter-probe binding site (Fig. 1D). To examine the effect of mutations on the anchor probe, we genotyped a patient with a heterozygous [XXIX] mutation using primer/probe set G (Fig. 3F). We found no change in the melting curves between the wild-type allele and the [XXIX] allele, thereby suggesting that point mutations within the anchor probe sequence have little effect on the melting curve analysis.

3.2. Validation

The genotypes determined at Tohoku University using the proposed method and those determined at Kagoshima University using a previously published method were identical for the 11 common mutations (Table S1 in supplementary material). We performed a similar test using DNA samples purified from filter-paper blood samples to determine if this method could be used for newborn screening. The genotypes determined in both laboratories were identical for all 26 DNA samples (Table S2 in supplementary material).

3.3. Frequency of eleven prevalent mutations

We found four heterozygous carriers of mutation [I], three of mutation [II], and two of mutation [V]. In addition, primer/probe set G detected one heterozygous mutation, which was confirmed as mutation [VIII] by direct sequencing. Altogether, 10 mutations were detected in 420 Japanese healthy controls.

4. Discussion

We developed a simple and rapid genetic test using real-time PCR combined with the HybProbe system for the 11 prevalent mutations in *SLC25A13*: mutations [I], [II], [III], [IV], [V], [VI], [VII], [VIII], [IX], [XIX], and [XXI]. This genetic test is a closed-tube assay in which no post-PCR handling of the samples is required. In addition, the genotyping is completed within 1 h. This test can utilize DNA samples purified from both peripheral blood and filter-paper blood. The reliability of the test was confirmed by genotyping 76 blind DNA samples from patients with citrin deficiency, including 50 peripheral blood and 26 filter-paper blood DNA samples. Because screening for the 11 targeted mutations would identify 95% of mutant alleles in the Japanese population [19], both, one, and no mutant alleles are expected to be identified in 90.4%, 9.3%, and less than 0.3% of patients, respectively. This genetic test would be useful not only in Japan but also other East Asian countries, including China, Korea, Taiwan and Vietnam, in which the same mutations are prevalent. Our test is expected to detect 76–87% of the mutant alleles in the Chinese population [12,19,25], 95–100% in the Korean population [12,19,26], 60–68% in the Taiwanese population [27,28], and 100% in the Vietnamese population [12,19]. If we were to prepare a primer/probe set for mutation [X]:g.IVS6+5G>A [12], which is prevalent in Taiwan, the estimated sensitivity would exceed 90% in the Taiwanese population [27,28].

Recently, the high resolution melting (HRM) method was reported to be suitable for the screening of mutations in the diagnosis of citrin deficiency [28]. HRM analysis is a closed-tube assay that screens for any base changes in the amplicons. The presence of SNPs anywhere on the amplicons can affect the melting curve, thereby suggesting that HRM is not suitable for screening for known mutations, but rather, is best suited to screening for unknown mutations. When we detected one heterozygous prevalent mutation, we performed HRM screening for all 17 exons of *SLC25A13*. After HRM screening, only the HRM-positive exons were subjected to direct sequencing analysis. Several mutant alleles were identified using this approach.

The frequency of homozygotes, including compound heterozygotes, presenting *SLC25A13* mutations in the population at Kagoshima (a prefecture in the southern part of Japan) has been calculated to be 1/17,000 based on the carrier rate (1/65) [19]. The prevalence of NICCD has been also reported to be 1/17,000–34,000 [29]. In this study, the carrier rate in Miyagi (a prefecture in northern Japan) was 1/42 (95% confidential interval, 1/108–1/26), thereby yielding an estimated frequency of patients with citrin deficiency of 1/7,100. Our result, together with the previous report [19], suggests that a substantial fraction of the homozygotes or compound heterozygotes of SLC25A13 mutations was asymptomatic during the neonatal period.

The early and definitive diagnosis of citrin deficiency may be beneficial for patients with citrin deficiency by encouraging specific dietary habits and avoiding iatrogenic worsening of brain edema by glycerol infusion when patients develop encephalopathy [30,31]. Because the screening of blood citrulline levels by tandem mass analysis at birth does not detect all patients with citrin deficiency, the development of a genetic test would be welcomed. In this study, we demonstrated that genomic DNA extracted from filter paper blood samples was correctly genotyped, thereby indicating the feasibility of newborn screening using this genetic test. If 100,000 babies in the northern part of Japan were screened by this method, we would detect 14 homozygotes or compound heterozygotes with *SLC25A13* mutations and 2400 heterozygous carriers. In 2400 heterozygous carriers, we would expect to observe only 1 to 2 compound heterozygotes with one target and one non-target mutation. The estimated frequency of babies with two non-target mutations is 0.04/100,000. Our genetic method would therefore allow us to screen newborn babies efficiently. If we performed this genetic test in a high-throughput real-time PCR system, such as a 384- or 1,536-well format, the cost per sample could be lowered.

In conclusion, we have established a rapid and simple detection system using the HybProbe assay for the 11 prevalent mutations in *SLC25A13*. This system could be used to screen newborns for citrin deficiency and may facilitate the genetic diagnosis of citrin deficiency, especially in East Asian populations.

Supplementary materials related to this article can be found online at doi:10.1016/j.ymgme.2011.12.024.

Acknowledgments

The authors acknowledge the contribution of Dr. Keiko Kobayashi, who passed away on December 21th, 2010. Dr. Kobayashi discovered that the *SLC25A13* gene is responsible for citrin deficiency and devoted much of her life to elucidating the mechanism of citrin deficiency. This work was supported by grants from the Ministry of Education, Culture, Sports, Science, and Technology and the Ministry of Health, Labor, and Public Welfare.

References

[1] K. Kobayashi, D.S. Sinasac, M. Iijima, A.P. Boright, L. Begum, J.R. Lee, T. Yasuda, S. Ikeda, R. Hirano, H. Terazono, M.A. Crackower, I. Kondo, L.C. Tsui, S.W. Scherer, T. Saheki, The gene mutated in adult-onset type II citrullinaemia encodes a putative mitochondrial carrier protein, Nat. Genet. 22 (1999) 159–163.

[2] T. Ohura, K. Kobayashi, Y. Tazawa, I. Nishi, D. Abukawa, O. Sakamoto, K. Iinuma, T. Saheki, Neonatal presentation of adult-onset type II citrullinemia, Hum. Genet. 108 (2001) 87–90.

[3] Y. Tazawa, K. Kobayashi, T. Ohura, D. Abukawa, F. Nishinomiya, Y. Hosoda, M. Yamashita, I. Nagata, Y. Kono, T. Yasuda, N. Yamaguchi, T. Saheki, Infantile cholestatic jaundice associated with adult-onset type II citrullinemia, J. Pediatr. 138 (2001) 735–740.

[4] T. Tomomasa, K. Kobayashi, H. Kaneko, H. Shimura, T. Fukusato, M. Tabata, Y. Inoue, S. Ohwada, M. Kasahara, Y. Morishita, M. Kimura, T. Saheki, A. Morikawa, Possible clinical and histologic manifestations of adult-onset type II citrullinemia in early infancy, J. Pediatr. 138 (2001) 741–743.

[5] T. Shigeta, M. Kasahara, T. Kimura, A. Fukuda, K. Sasaki, K. Arai, A. Nakagawa, S. Nakagawa, K. Kobayashi, S. Soneda, H. Kitagawa, Liver transplantation for an

infant with neonatal intrahepatic cholestasis caused by citrin deficiency using heterozygote living donor, Pediatr. Transplant. 14 (2009) E86–88.
[6] M. Kasahara, S. Ohwada, T. Takeichi, H. Kaneko, T. Tomomasa, A. Morikawa, K. Yonemura, K. Asonuma, K. Tanaka, K. Kobayashi, T. Saheki, I. Takeyoshi, Y. Morishita, Living-related liver transplantation for type II citrullinemia using a graft from heterozygote donor, Transplantation 71 (2001) 157–159.
[7] Y. Takashima, M. Koide, H. Fukunaga, M. Iwai, M. Miura, R. Yoneda, T. Fukuda, K. Kobayashi, T. Saheki, Recovery from marked altered consciousness in a patient with adult-onset type II citrullinemia diagnosed by DNA analysis and treated with a living related partial liver transplantation, Intern. Med. 41 (2002) 555–560.
[8] A. Tamamori, Y. Okano, H. Ozaki, A. Fujimoto, M. Kajiwara, K. Fukuda, K. Kobayashi, T. Saheki, Y. Tagami, T. Yamano, Neonatal intrahepatic cholestasis caused by citrin deficiency: severe hepatic dysfunction in an infant requiring liver transplantation, Eur. J. Pediatr. 161 (2002) 609–613.
[9] T. Ohura, K. Kobayashi, Y. Tazawa, D. Abukawa, O. Sakamoto, S. Tsuchiya, T. Saheki, Clinical pictures of 75 patients with neonatal intrahepatic cholestasis caused by citrin deficiency (NICCD), J. Inherit. Metab. Dis. 30 (2007) 139–144.
[10] T. Yasuda, N. Yamaguchi, K. Kobayashi, I. Nishi, H. Horinouchi, M.A. Jalil, M.X. Li, M. Ushikai, M. Iijima, I. Kondo, T. Saheki, Identification of two novel mutations in the SLC25A13 gene and detection of seven mutations in 102 patients with adult-onset type II citrullinemia, Hum. Genet. 107 (2000) 537–545.
[11] N. Yamaguchi, K. Kobayashi, T. Yasuda, I. Nishi, M. Iijima, M. Nakagawa, M. Osame, I. Kondo, T. Saheki, Screening of SLC25A13 mutations in early and late onset patients with citrin deficiency and in the Japanese population: identification of two novel mutations and establishment of multiple DNA diagnosis methods for nine mutations, Hum. Mutat. 19 (2002) 122–130.
[12] Y.B. Lu, K. Kobayashi, M. Ushikai, A. Tabata, M. Iijima, M.X. Li, L. Lei, K. Kawabe, S. Taura, Y. Yang, T.-T. Liu, S.-H. Chiang, K.-J. Hsiao, Y.-L. Lau, L.-C. Tsui, D.H. Lee, T. Saheki, Frequency and distribution in East Asia of 12 mutations identified in the SLC25A13 gene of Japanese patients with citrin deficiency, J. Hum. Genet. 50 (2005) 338–346.
[13] E. Ben-Shalom, K. Kobayashi, A. Shaag, T. Yasuda, H.-Z. Gao, T. Saheki, C. Bachmann, O. Elpeleg, Infantile citrullinemia caused by citrin deficiency with increased dibasic amino acids, Mol. Genet. Metab. 77 (2002) 202–208.
[14] J. Takaya, K. Kobayashi, A. Ohashi, M. Ushikai, A. Tabata, S. Fujimoto, F. Yamato, T. Saheki, Y. Kobayashi, Variant clinical courses of 2 patients with neonatal intrahepatic cholestasis who have a novel mutation of SLC25A13, Metab. Clin. Exp. 54 (2005) 1615–1619.
[15] A. Luder, A. Tabata, M. Iijima, K. Kobayashi, H. Mandel, Citrullinaemia type 2 outside East Asia: Israeli experience, J. Inherit. Metab. Dis. 29 (2006) 59.
[16] T. Hutchin, M. Preece, K. Kobayashi, T. Saheki, R. Brown, D. Kelly, P. McKiernan, A. Green, U. Baumann, Neonatal intrahepatic cholestasis caused by citirn deficiency (NICCD) in a European patient, J. Inherit. Metab. Dis. 29 (2006) 112.
[17] J.-S. Sheng, M. Ushikai, M. Iijima, S. Packman, K. Weisiger, M. Martin, M. McCracken, T. Saheki, K. Kobayashi, Identification of a novel mutation in a Taiwanese patient with citrin deficiency, J. Inherit. Metab. Dis. 29 (2006) 163.
[18] J.M. Ko, G.-H. Kim, J.-H. Kim, J.Y. Kim, J.-H. Choi, M. Ushikai, T. Saheki, K. Kobayashi, H.-W. Yoo, Six cases of citrin deficiency in Korea, Int. J. Mol. Med. 20 (2007) 809–815.
[19] A. Tabata, J.-S. Sheng, M. Ushikai, Y.-Z. Song, H.-Z. Gao, Y.-B. Lu, F. Okumura, M. Iijima, K. Mutoh, S. Kishida, T. Saheki, K. Kobayashi, Identification of 13 novel mutations including a retrotransposal insertion in SLC25A13 gene and frequency of 30 mutations found in patients with citrin deficiency, J. Hum. Genet. 53 (2008) 534–545.
[20] P.S. Bernard, R.S. Ajioka, J.P. Kushner, C.T. Wittwer, Homogeneous multiplex genotyping of hemochromatosis mutations with fluorescent hybridization probes, Am. J. Pathol. 153 (1998) 1055–1061.
[21] C.N. Gundry, P.S. Bernard, M.G. Herrmann, G.H. Reed, C.T. Wittwer, Rapid F508del and F508C assay using fluorescent hybridization probes, Genet. Test. 3 (1999) 365–370.
[22] T. Saheki, K. Kobayashi, I. Inoue, Hereditary disorders of the urea cycle in man: biochemical and molecular approaches, Rev. Physiol. Biochem. Pharmacol. 108 (1987) 21–68.
[23] K. Kobayashi, M. Horiuchi, T. Saheki, Pancreatic secretory trypsin inhibitor as a diagnostic marker for adult-onset type II citrullinemia, Hepatology 25 (1997) 1160–1165.
[24] Y. Tazawa, K. Kobayashi, D. Abukawa, I. Nagata, S. Maisawa, R. Sumazaki, T. Iizuka, Y. Hosoda, M. Okamoto, J. Murakami, S. Kaji, A. Tabata, Y.B. Lu, O. Sakamoto, A. Matsui, S. Kanzaki, G. Takada, T. Saheki, K. Iinuma, T. Ohura, Clinical heterogeneity of neonatal intrahepatic cholestasis caused by citrin deficiency: case reports from 16 patients, Mol. Genet. Metab. 83 (2004) 213–219.
[25] H.Y. Fu, S.R. Zhang, X.H. Wang, T. Saheki, K. Kobayashi, J.S. Wang, The mutation spectrum of the SLC25A13 gene in Chinese infants with intrahepatic cholestasis and aminoacidemia, J. Gastroenterol. 46 (2011) 510–518.
[26] K. Kobayashi, Y.B. Lu, M.X. Li, I. Nishi, K.-J. Hsiao, K. Choeh, Y. Yang, W.-L. Hwu, J.K.V. Reichardt, F. Palmieri, Y. Okano, T. Saheki, Screening of nine SLC25A13 mutations: their frequency in patients with citrin deficiency and high carrier rates in Asian populations, Mol. Genet. Metab. 80 (2003) 356–359.
[27] T. Saheki, K. Kobayashi, M. Iijima, M. Horiuchi, L. Begum, M.A. Jalil, M.X. Li, Y.B. Lu, M. Ushikai, A. Tabata, M. Moriyama, K.-J. Hsiao, Y. Yang, Adult-onset type II citrullinemia and idiopathic neonatal hepatitis caused by citrin deficiency: involvement of the aspartate glutamate carrier for urea synthesis and maintenance of the urea cycle, Mol. Genet. Metab. 81 (Suppl 1) (2004) S20–S26.
[28] J.T. Lin, K.J. Hsiao, C.Y. Chen, C.C. Wu, S.J. Lin, Y.Y. Chou, S.C. Shiesh, High resolution melting analysis for the detection of SLC25A13 gene mutations in Taiwan, Clin. Chim. Acta 412 (2011) 460–465.
[29] Y. Shigematsu, S. Hirano, I. Hata, Y. Tanaka, M. Sudo, N. Sakura, T. Tajima, S. Yamaguchi, Newborn mass screening and selective screening using electrospray tandem mass spectrometry in Japan, J. Chromatogr. B Analyt. Technol. Biomed. Life Sci. 776 (2002) 39–48.
[30] M. Yazaki, Y.-i. Takei, K. Kobayashi, T. Saheki, S.-I. Ikeda, Risk of worsened encephalopathy after intravenous glycerol therapy in patients with adult-onset type II citrullinemia (CTLN2), Intern. Med. 44 (2005) 188–195.
[31] H. Takahashi, T. Kagawa, K. Kobayashi, H. Hirabayashi, M. Yui, L. Begum, T. Mine, S. Takagi, T. Saheki, Y. Shinohara, A case of adult-onset type II citrullinemia—deterioration of clinical course after infusion of hyperosmotic and high sugar solutions, Med. Sci. Monit. 12 (2006) CS13–CS15.

Please cite this article as: A. Kikuchi, et al., Simple and rapid genetic testing for citrin deficiency by screening 11 prevalent mutations in *SLC25A13*, Mol. Genet. Metab. (2012), doi:10.1016/j.ymgme.2011.12.024

Eur J Pediatr (2012) 171:301–305
DOI 10.1007/s00431-011-1534-2

ORIGINAL PAPER

Proportion of malformations and genetic disorders among cases encountered at a high-care unit in a children's hospital

Akiko Soneda · Hideki Teruya · Noritaka Furuya · Hiroshi Yoshihashi · Keisuke Enomoto · Aki Ishikawa · Kiyoshi Matsui · Kenji Kurosawa

Received: 5 May 2011 / Accepted: 5 July 2011 / Published online: 16 July 2011

Abstract Genetic disorders and birth defects account for a high percentage of the admissions in children's hospitals. Congenital malformations and chromosomal abnormalities are the most common causes of infant mortality. So their effects pose serious problems for perinatal health care in Japan, where the infant mortality is very low. This paper describes the reasons for admissions and hospitalization at the high-care unit (HCU) of a major tertiary children's referral center in Japan. We retrospectively reviewed 900 admission charts for the period 2007–2008 and found that genetic disorders and malformations accounted for a significant proportion of the cases requiring admission to the HCU. Further, the rate of recurrent admission was higher for patients with genetic disorders and malformations than for those with acquired, non-genetic conditions. Over the past 30 years, admissions attributed to genetic disorders and malformations has consistently impacted on children's hospital and patients with genetic disorders and malformations form a large part of this facility. These results reflect improvements in medical care for patients with genetic disorders and malformations and further highlight the large proportion of cases with genetic disorders, for which highly specialized management is required. Moreover, this study emphasizes the need for involvement of clinical geneticists in HCUs at children's hospitals.

Keywords Malformation · Genetic disease · High-care unit · Children's hospital · Mortality

Grant sponsor The Ministry of Health, Labor and Welfare, Japan

A. Soneda · N. Furuya · H. Yoshihashi · K. Enomoto · A. Ishikawa · K. Kurosawa (✉)
Division of Medical Genetics,
Kanagawa Children's Medical Center,
2-138-4 Mutsukawa, Minami-ward,
Yokohama 232-8555, Japan
e-mail: kkurosawa@kcmc.jp

H. Teruya
Division of Critical Care Medicine,
Kanagawa Children's Medical Center,
Yokohama, Japan

K. Matsui
Division of General Pediatrics,
Kanagawa Children's Medical Center,
Yokohama, Japan

H. Teruya
Department of Pediatrics, Yokohama Rosai Hospital,
Yokohama, Japan

K. Kurosawa
Clinical Research Institute, Kanagawa Children's Medical Center,
Yokohama, Japan

Introduction

Genetic disorders and birth defects account for a high percentage of the admissions to children's hospitals [4, 13]. In 2008 [5], the Ministry of Health, Labor and Welfare in Japan reported that congenital malformations, chromosomal abnormalities, and genetic diseases are the leading causes of death in children during the first year of life. As per that report, 999 infants under the age of 1 year died of congenital malformations and chromosomal abnormalities; this corresponds to 35.7% of the total number of deaths in this age group. Since 1985, congenital malformations and chromosomal abnormalities have remained the leading causes of infant mortality in Japan [5]. Indeed, in USA it

has been found that patients with genetic disorders had a greater need for hospital admission and were hospitalized for longer durations than were those without genetic disorders [14].

However, recent advances in treatment are likely to improve the survival of individuals with congenital malformations, which, in turn, is likely to increase the rates of readmission to pediatric intensive care units (PICUs) [16]. Several studies have assessed the role of genetic disorders in pediatric mortality and hospitalization [2, 6, 7, 16]. Congenital malformations and chromosomal abnormalities pose serious challenges for perinatal health care in this country, as they are the leading contributors to the infant mortality rate in Japan.

In this study, we assessed the reasons for admissions and hospitalization to the high-care unit (HCU) of a major tertiary children's referral center in Kanagawa Prefecture, Japan, and compared our findings to those of a study of this unit 30 years ago. To elucidate the impact and contribution of birth defects and genetic diseases on pediatric hospitalization, we studied the reason for hospitalization, underlying diagnoses, and duration of hospitalization in this children's hospital in Japan.

Materials and methods

Permission for the study was obtained from the Ethical Committee of our medical center.

We retrospectively analyzed the cases of children hospitalized at the HCU of Kanagawa Children's Medical Center (KCMC) between June 2007 and December 2008. KCMC is a major tertiary children's referral center for pediatric cardiology, surgery, and cancer cases and serves a large area in Kanagawa Prefecture, Japan. It has an institute for the severely handicapped, a PICU, a neonatal intensive care unit, and an HCU. In contrast to the PICU, which admits patients who have undergone cardiovascular or neurosurgery, the HCU specializes in pediatric patients with other acute conditions. All of the patients were included if they were admitted to the HCU from the emergency room, operating room, or inpatient ward. KCMC, with 419 beds, is the only specialized pediatric hospital in Kanagawa Prefecture, where the total number of births is 80,000 annually [8, 9]. About 8,500 patients (male/female, 1:1) were admitted to KCMC in 2007, and the average of hospital stay was 15.3 days.

We summarized and reviewed the medical charts of all patients admitted to the HCU. The charts and summaries were reviewed for age, sex, duration of hospitalization, underlying disease, and reason for admission. Subcategories were created for the underlying diseases and reason for admission.

The underlying disease was classified into two main categories: genetic conditions and acquired (non-genetic) conditions. Genetic conditions were considered to include chromosomal abnormalities, recognizable malformation and dysplasia, multiple malformations, isolated malformations (e.g., those related to the heart, central nervous system (CNS), and respiratory and gastrointestinal tracts), other single-gene defect-related conditions, mitochondrial diseases, and metabolic disorders (Table 1). All cases of chromosomal abnormalities and multiple malformations were examined using standard karyotyping. Cases of recognizable malformation/dysplasia were ascertained by clinical dysmorphologists (H.Y., N.F., and K.K.). Acquired conditions were considered to include perinatal complications, trauma, neoplasm, and sequelae of severe infectious conditions.

The reasons for admission were classified as problems of the respiratory system, CNS, heart, gastrointestinal tract, kidneys and urinary tract, infectious diseases, post-operative management, and unknown condition. Those cases that did not fall into these categories were placed into a category called "others."

Statistical analyses were performed to compare the duration of hospitalization and the age distribution, using StatView version 5.0 (SAS Institute, Inc; Cary, NY). Categorical data were reported as counts and percentages, and continuous data as mean (SD) or median values. Statistical differences for categorical variables were determined by using chi-squared analyses. Median differences were compared by Mann–Whitney *U* test.

Results

A total of 900 admissions, consisting of 687 individual cases with 200 recurrent admissions, were reviewed. Sixteen admissions were excluded from the study because of insufficient information regarding the underlying causes for admission.

The median age at admission was 3.5 years (range, 1 day–32.5 years), and the sex ratio was 1.36 (396 males and 291 females). The median lengths of hospitalization in the HCU were 4 days. Table 2 shows the distribution of the 884 admissions across the different categories of causes for admission. Most patients were admitted for common medical problems, including respiratory problems, post-operative management, and CNS problems. Of the 298 admissions for respiratory problems, most cases involved respiratory infection, including pneumonia and bronchitis. Admissions for post-operative management accounted for 30.7% cases (271 of 884 admissions), while CNS problems such as convulsions, encephalitis, and meningitis accounted for 16.3% (144 of 884 admissions).

Table 1 Definitions of categories

Category	Examples
Chromosomal syndromes	Down syndrome, trisomies 13 and 18, cri du chat syndrome, and Wolf–Hirschhorn syndrome
Recognizable malformation/dysplasia	22q11.2 deletion syndrome, CHARGE syndrome, and VATER association, Lowe syndrome, achondroplasia, Crouzon syndrome, Noonan syndrome, and Treacher–Collins syndrome
Multiple malformations	
Isolated malformations	
Congenital heart diseases	VSD ASD, AVSD, TGA, and DORV
Central nervous system malformations	Schistorrhachis, hydrocephalus, and meningoencephalocele
Gastrointestinal malformations	Diaphragmatic hernia, biliary atresia, and congenital intestinal obstruction
Respiratory system malformations	CCAM and tracheal stenosis
Other isolated malformations	Cleft palate and cleft lip
Single-gene defect	Metabolic diseases, spinal muscular atrophy, and spinocerebellar degeneration
Mitochondrion	

The classification of the underlying conditions of the 687 patients is shown in Table 3. In 13 cases, the data for identifying the underlying disease were insufficient (e.g., charts were missing). These cases were categorized as "unknown condition." Of the total 687 patients, 372 (54.1%) had genetic disorders and the remaining 302 (44.0%) had acquired conditions unrelated to genetic disorders, including perinatal complications, neoplasm, and trauma. Among the 372 patients with genetic disorders, 72 had chromosomal abnormalities, with Down syndrome (29 cases) being the most common underlying disorder. Seventy patients had recognizable malformations and dysplasia, with conditions such as osteogenesis imperfecta, 22q11.2 deletion syndromes, CHARGE syndrome, and VATER association. Multiple malformations with unrecognizable patterns were present in 38 cases while isolated malformations, including CNS malformation, congenital heart disease, and gastrointestinal malformation were present in 160 cases.

We also summarized the reasons for the total of 884 admissions, according to the underlying condition (genetic or acquired). Of these admissions, 200 were readmissions. Patients with genetic disorders and malformations had a greater tendency to be hospitalized repeatedly as compared with those with acquired conditions (Fig. 1). In both genetic and acquired condition categories, respiratory disease, post-operative management, and CNS problems were the major medical problems leading to admission.

We further compared age distribution and the lengths of hospitalization between the groups with genetic and acquired disorders (Table 4). The patients with genetic

Table 2 Medical problems for admission (N=884)

Causes for admission	Number	Percent
Respiratory problems	298	33.7
Post-operative management	271	30.7
CNS problems	144	16.3
Gastrointestinal problems	35	4.0
Cardiac diseases	23	2.6
Other infectious state	23	2.6
Examination	21	2.4
Kidney and urinary tract problems	14	1.6
Other	55	6.2
Total	884	100.0

Table 3 Classification of underlying diseases in 678 patients

Underlying diseases	Number	Percent
Genetic disorders and malformations (subtotal)	372	54.1
Chromosomal abnormalities	(72)	10.5
Recognizable malformation/dysplasia	(70)	10.2
Multiple malformations	(38)	5.5
Isolated malformations	(subtotal:160)	23.3
Central nervous system malformation	(71)	10.3
Congenital heart disease	(35)	5.1
Gastrointestinal malformation	(32)	4.7
Respiratory system malformation	(9)	1.3
Other isolated malformations	(13)	1.9
Single-gene defect	(26)	3.8
Mitochondrion	(6)	0.9
Acquired non-genetic conditions (subtotal)	302	44.0
Perinatal complications	(66)	9.6
Neoplasm	(38)	5.5
Trauma(non-accidental and accidental)	(27)	3.9
Infection	(16)	2.3
Other	(155)	22.6
Unknown	13	1.9
Total	687	100.0

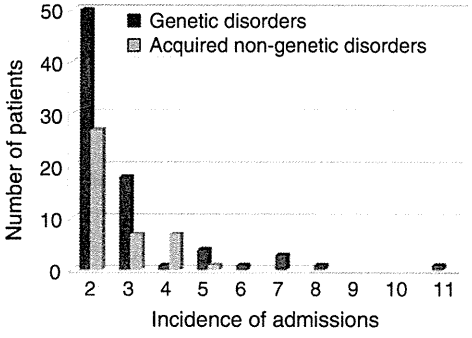

Fig. 1 Comparison of the incidence of admission between the groups with genetic disorders and acquired disorders. In both groups, a total of 200 patients were readmitted. The group with genetic disorders generally required frequent readmission

disorders were significantly younger than those with acquired conditions (median age, 2.0 vs. 4.9 years; $P<0.0001$). There is no significant difference in the length of hospitalization between the patients with genetic disorders and those with acquired conditions (median, 4 vs. 4 days; $P=0.26$), but some patients with genetic disorders had much longer hospitalization (mean, 13.0 vs. 7.0 days; $P=0.007$; range, 1–979 days). Among the reasons for admission, respiratory problems tended to have a longer duration of hospitalization for patients with genetic disorders than for those with acquired conditions (median, 7 vs. 5 days; $P=0.17$).

Discussion

Our study shows that genetic disorders and malformations account for a significant proportion of cases requiring admission to the HCU. Additionally, the rate of recurrent admission was higher among patients with genetic disorders and malformations than among those with acquired non-genetic conditions. This finding is in agreement with those of previous reports for other countries [4, 13].

Several studies from different countries have previously suggested that genetic conditions and malformations and the associated mortality and morbidity have a significant impact on the cost burden for society and the patients' families. Cunniff et al. reported that 19% of deaths in a PICU were in cases of heritable disorders [1]. Stevenson and Carey reported that the 34.4% of deaths in a children's hospital were due to malformations and genetic disorders [15]. On the basis of a population-based study, Yoon et al. reported that the overall rate of hospitalization was related to birth defects and genetic diseases, and varied with age and race/ethnicity [16]. McCandless et al. reported the enormous impact of genetic disease on inpatient pediatrics and the health care system in both admission rates and the total hospital charges [11]. These studies emphasize the importance of understanding the impact that genetic diseases have on mortality and healthcare strategies [15]. Furthermore, it is also clear that early recognition of the underlying disorders is necessary for optimal management of patients with genetic disorders.

Our study highlights another aspect related to the impact of genetic disorders and malformations. In 1981, Matsui et al. analyzed the cases of 18,736 children of total admission during 1975–1979 to KCMC and found that 44% had genetic disorders and malformations [10]. Although our study period and ward are limited to those in the HCU, the patients with genetic disorders and malformations had consistently significant impact in KCMC during the ensuing three decades. Further, it emphasizes that medical care for acute conditions and surgical procedures frequently requires highly specialized knowledge of unusual disease conditions and should be provided in consultation with specialists such as clinical geneticists.

Table 4 Comparison of patients with genetic disorder vs. acquired condition on ages at admission and lengths of stay

	Genetic disorders		Acquired conditions		
	Median (range)	*n*	Median (range)	*n*	*P*
Ages	2.0 years (1 day–27.0 years)	372*	4.9 years (9 days–32.5 years)	302*	<0.0001
Length of hospitalization (days)					
Respiratory problem	7 (1–979)	182	5 (1–97)	109	0.17
CNS	4 (1–54)	73	4 (1–207)	68	0.61
Cardiovascular	4 (2–11)	13	4 (2–24)	8	0.94
Gastrointestinal	5.5 (1–37)	22	5 (2–15)	12	0.60
Kidney and urinary tract	3 (2–12)	5	8 (2–12)	9	0.32
Sepsis	3.5 (2–9)	14	7 (2–20)	9	0.19
Post-operative care	2 (1–49)	174	2 (1–62)	93	0.18
Total	4 (1–979)	518	4 (1–207)	366	0.26

*For the patients who have recurrent admissions, the only first admission was calculated

Although the strategies for management of respiratory infection, by means of newly developed antibiotics and mechanical ventilators, and surgical intervention for infants with malformations, have improved, the general strategies for the medical treatment of genetic disorders and malformations remain to be clarified. Hall commented on the report by Yoon et al. [16] and emphasized the significance of basic research on the human genome and developmental genetics [3]. As shown in Table 2, genetic disorders and malformations include rare diseases, which, although uncommon, remain an important public-health issue and a challenge for the medical community [12].

Our study had the limitations of genetic studies and evaluation in cases with multiple malformations and other isolated malformations. The underlying conditions of most patients in this study were ascertained by clinical geneticists, but high-resolution genome analysis with arrays using comparative genomic hybridization was applied in only limited cases. Recently, research attention has focused to a large extent on rare genetic disorders and Mendelian diseases, because of their significant effect on human health, with the aim of identifying disease-related genetic variations. Re-evaluation and classification of underlying disorders, especially in the case of multiple congenital anomalies in undiagnosed patients, are required for further analysis.

Another limitation of our study is estimation of the financial burden of the group of patients with a genetic background. McCandless et al. showed that the disorders with genetic determinant account for 81% of the total hospital charges [11]. Their results are consistent with those of Hall et al. in 1978 [4]. Further analysis of financial burden in our study may provide useful information for improvement of health care systems.

In conclusion, we report here the proportion of genetic disorders and malformations among cases encountered at the HCU of a tertiary children's medical center in Japan. Over 30 years, the proportion of admissions attributed to genetic disorders and malformations has impact and currently accounts for more than half of admissions to this facility. These results firstly indicate improvements in medical care for patients with genetic disorders and malformations and further highlight the large proportion of cases with genetic disorders. As these cases require highly specialized management, the involvement of clinical geneticists in HCUs at children's hospitals is crucial. Eventually, a better fundamental understanding of genetic disorders and malformations may lead to further improvements in medical care and may reduce the impact of these conditions on the patients and their families.

Acknowledgments The authors are grateful to Dr. Hiroyuki Ida (Tokyo Jikei University) for his valuable comments. This research was supported in part by a grant-in-aid from the Ministry of Health, Labor and Welfare, Japan.

Conflict of interest The authors declare no conflict of interest.

References

1. Cunniff C, Carmack JL, Kirby RS, Fiser DH (1995) Contribution of heritable disorders to mortality in the pediatric intensive care unit. Pediatrics 95:678–681
2. Garrison MM, Jeffries H, Christakis DA (2005) Risk of death for children with Down syndrome and sepsis. J Pediatr 147:748–752
3. Hall JG (1997) The impact of birth defects and genetic diseases. Arch Pediatr Adolesc Med 151:1082–1083
4. Hall JG, Poweres EK, McIlvaine RT, Ean VH (1978) The frequency and financial burden of genetic disease in a pediatric hospital. Am J Med Genet 1:417–436
5. Health and Welfare Statistics Association (2010) Mortality rate of infant. J Health Welfare Statist 57:63–65, in Japanese
6. Heron M, Sutton PD, Xu J, Vetura SJ, Strobino DM, Guyer B (2010) Annual summary of vital statistics: 2007. Pediatrics 125:4–15
7. Hudome SM, Kirby RS, Senner JW, Cunniff C (1994) Contribution of genetic disorders to neonatal mortality in a regional intensive care setting. Am J Perinatol 11:100–103
8. Kuroki Y, Konishi H (1984) Current status and perspectives in the Kanagawa Birth Defects Monitoring Program (KAMP). Cong Anom 24:385–393
9. Kurosawa K, Imaizumi K, Masuno M, Kuroki Y (1994) Epidemiology of limb-body wall complex in Japan. Am J Med Genet 51:143–146
10. Matsui I, Naito K, Hanawa Y et al (1981) Impact of the congenital birth defects on children's health care. J Jpn Pediatr Soc 85:889–897, in Japanese
11. McCandless SE, Brunger JW, Cassidy SB (2004) The burden of genetic disease on inpatient care in a children's hospital. Am J Hum Genet 74:121–127
12. Schieppati A, Henter J-I, Daina E, Aperia A (2008) Why rare diseases are an important medical and social issue. Lancet 371:2039–2041
13. Scriver CR, Neal JL, Saginur R, Clow A (1973) The frequency of genetic disease and congenital malformation among patients in a pediatric hospital. Can Med Assoc J 108:1111–1115
14. Sever L, Lynberg MC, Edmonds LD (1993) The impact of congenital malformations on public health. Teratology 48:547–549
15. Stevenson DA, Carey JC (2004) Contribution of malformations and genetic disorders to mortality in a children's hospital. Am J Med Genet 126A:393–397
16. Yoon PW, Olney RS, Khoury MJ, Sappenfield WM, Chavez GF, Taylor D (1997) Contribution of birth defects and genetic diseases to pediatric hospitalizations. Arch Pediatr Adolesc Med 151:1096–1103

Hum Genet (2012) 131:99–110
DOI 10.1007/s00439-011-1047-0

ORIGINAL INVESTIGATION

Novel intragenic duplications and mutations of *CASK* in patients with mental retardation and microcephaly with pontine and cerebellar hypoplasia (MICPCH)

Shin Hayashi · Nobuhiko Okamoto · Yasutsugu Chinen · Jun-ichi Takanashi · Yoshio Makita · Akira Hata · Issei Imoto · Johji Inazawa

Received: 16 December 2010 / Accepted: 15 June 2011 / Published online: 7 July 2011

Abstract The *CASK* gene encoding a member of the membrane-associated guanylate kinase protein family is highly expressed in the mammalian nervous system of both adults and fetuses, playing several roles in neural development and synaptic function. Recently, *CASK* aberrations caused by both mutations and deletions have been reported to cause severe mental retardation (MR), microcephaly and disproportionate pontine and cerebellar hypoplasia (MICPCH) in females. Here, mutations and copy numbers of *CASK* were examined in ten females with MR and MICPCH, and the following changes were detected: nonsense mutations in three cases, a 2-bp deletion in one case, mutations at exon–intron junctions in two cases, heterozygous deletions encompassing *CASK* in two cases and interstitial duplications in two cases. Except for the heterozygous deletions, each change including the intragenic duplications potentially caused an aberrant transcript, resulting in *CASK* null mutations. The results provide novel mutations and copy number aberrations of *CASK*, causing MR with MICPCH, and also demonstrate the similarity of the phenotypes of MR with MICPCH regardless of the *CASK* mutation.

Introduction

The *CASK* gene (OMIM: *300172) encoding a member of the membrane-associated guanylate kinase (MAGUK) protein family is highly expressed in the mammalian ner-

Electronic supplementary material The online version of this article (doi:10.1007/s00439-011-1047-0) contains supplementary material, which is available to authorized users.

S. Hayashi · I. Imoto · J. Inazawa (✉)
Department of Molecular Cytogenetics, Medical Research Institute and School of Biomedical Science, Tokyo Medical and Dental University, 1-5-45 Yushima, Bunkyo-ku, Tokyo 113-8510, Japan
e-mail: johinaz.cgen@mri.tmd.ac.jp

S. Hayashi
Hard Tissue Genome Research Center, Tokyo Medical and Dental University, Tokyo, Japan

N. Okamoto
Department of Planning and Research, Osaka Medical Center and Research Institute for Maternal and Child Health, Osaka, Japan

Y. Chinen
Department of Pediatrics, University of the Ryukyu School of Medicine, Okinawa, Japan

J. Takanashi
Department of Pediatrics, Kameda Medical Center, Chiba, Japan

Y. Makita
Education Center, Asahikawa Medical College, Asahikawa, Japan

A. Hata
Department of Public Health, Chiba University Graduate School of Medicine, Chiba, Japan

I. Imoto
Department of Human Genetics and Public Health Graduate School of Medical Science, The University of Tokushima, Tokushima, Japan

J. Inazawa
Global Center of Excellence (GCOE) Program for 'International Research Center for Molecular Science in Tooth and Bone Diseases', Tokyo Medical and Dental University, Tokyo, Japan

vous system of both adults and fetuses (Stevenson et al. 2000), and plays several roles in neural development and synaptic function (Hsueh 2006). Recently, we have reported the possible involvement of the decrease of intact *CASK* expression induced by a microdeletion at Xp11.4 in the pathogenesis of mental retardation (MR) and microcephaly (Hayashi et al. 2008). Concurrently, Najm et al. (2008) reported that mutations of *CASK* caused severe MR, microcephaly, and disproportionate pontine and cerebellar hypoplasia (MICPCH, OMIM: #300749). To examine the involvement of point mutations and/or copy number variations (CNVs) of *CASK* in patients with MR and MICPCH, we performed DNA sequencing and molecular cytogenetic analyses including array-based comparative genomic hybridization (aCGH) in ten patients showing such phenotypes. Pathogenic alterations of *CASK* were detected in all ten cases, and each change including intragenic duplications caused a truncation of the gene.

Subjects and methods

Subjects

From three hospitals in Japan, we recruited ten Japanese females (patients 1–10) suspected of having *CASK* mutations based on phenotypic criteria: female, MR and MICPCH. All patients were examined and evaluated by clinical dysmorphologists in each hospital. Their clinical features are shown in Table 1.

Briefly, their ages at the last follow-up ranged from 11 months to 14 years. All were born by normal full-term deliveries. At birth, patients 1, 2, 3, 5 and 7 revealed obvious signs of microcephaly (<−2.0 SD) and at present all the patients show severe microcephaly; their development has been markedly retarded. Only patients 5 and 6 can walk, and only patient 9 can speak any words at all. Patients 1, 2, 7, 9 and 10 show muscular hypotonia. Magnetic resonance imaging (MRI) of the brain demonstrated similar aberrations; all patients revealed hypoplasia of the cerebellum, mesencephalon and pons (Fig. 1; Table 1). Conventional karyotyping of peripheral blood lymphocytes with approximately 400–550 bands revealed a normal female karyotype, 46,XX, in each patient.

All samples were obtained with prior written informed consent from the parents and approval by the local ethics committee and all the institutions involved in this project. A lymphoblastoid cell line (LCL) was established by infecting lymphocytes of the patients and patients' parents with Epstein–Barr virus, as described previously (Saito-Ohara et al. 2002).

Mutation analysis

Mutations within all coding sequences of *CASK* were analyzed by exon amplification and direct sequencing using primer combinations designed for genomic sequences around each exon (Najm et al. 2008). Any base changes detected in samples were confirmed by sequencing each product in both directions.

aCGH analysis

For patients in whom no mutation of *CASK* was detected, we performed aCGH to estimate the genomic copy number variant (CNV) around *CASK*. We employed an in-house bacterial artificial chromosome (BAC)-based array, the 'MCG X-tiling array' (X-Array) (Inazawa et al. 2004), which contains 1001 BAC/PACs throughout the X-chromosome other than pseudoautosomal regions for aCGH analysis (Hayashi et al. 2007). Hybridization was performed as described elsewhere (Hayashi et al. 2007). For two patients, we also applied an oligonucleotide array (Agilent Human Genome CGH Microarray 244K; Agilent Technologies, Santa Clara, CA, USA) to determine the boundaries of the CNVs identified with the X-Array. DNA labeling, hybridization and washing of the arrays were performed according to the directions provided by the manufacturer. The hybridized arrays were scanned using an Agilent scanner (G2565BA), and the CGH Analytics program version 3.4.40 (Agilent Technologies) was used to analyze CNVs after data extraction, filtering and normalization by Feature Extraction software (Agilent Technologies).

Fluorescence in situ hybridization (FISH)

FISH was performed as described elsewhere (Hayashi et al. 2005) using BAC clones located around the region of interest to confirm all the detected CNVs.

Genomic PCR and reverse transcription-PCR

Genomic PCR was performed on genomic DNA of the ten patients and an unaffected female as a control. Reverse transcription-PCR (RT-PCR) was performed on cDNA extracted from LCLs of patients 5, 6, 9 and 10 and an unaffected female as a control. The sequences of the primer combinations are provided in Supplementary Table 1.

Real-time quantitative PCR

To determine the boundaries of the duplications more precisely, real-time quantitative PCR (qPCR) was performed

Table 1 Clinical features and analysis of *CASK*

Patient	1	2	3	4	5	6	7	8	9	10
Gender	F	F	F	F	F	F	F	F	F	F
Age at last follow-up	2 years, 8 months	2 years, 0 month	2 years, 8 months	11 months	7 years, 9 months	14 years	1 years, 9 months	2 years, 0 months	12 years	7 years, 2 months
Gestational age (weeks)	41	41	40	41	40	41	36	41	41	41
Height at birth (SD)	*NA*	0.2	−2.6	−0.8	−3.8	−0.8	−2.2	−0.9	−2.0	0.2
Weight at birth (SD)	−1.9	−0.1	−1.6	−0.7	−2.2	−0.3	−2.9	−1.9	−1.1	0.4
OFC at birth (SD)	−3.2	−2.3	−2.8	−0.8	−3.4	−0.4	−4.3	−1.3	−1.9	−1.5
Height at last follow-up (SD)	−1.5	−2.7	−1.9	−1.7	−3.7	−4.9	−0.9	−3.0	−3.5	−3.0
Weight at last follow-up (SD)	−2.5	−2.2	−2.1	−1.4	−2.4	−3.3	−2.0	−2.5	−2.3	−2.0
OFC at last follow-up (SD)	−4.3	−3.5	−4.0	−3.2	−4.5	−6	−4.6	−4	−5.4	−5.2
Mental retardation	Severe	Moderate	Severe	Severe	Severe	Moderate	Severe	Moderate	Severe	Severe
Development (month)										
Holding one's head	6	4	4	5	3	4	6	4	+	3
Sitting	–	9	–	–	12	9	12	15	–	22
Walking	–	–	–	–	36	30	–	–	–	–
Speech	–	–	–	–	–	–	–	A few words spoken	–	–
Muscular hypotonia	+	+	–	–	–	NA	+	–	+	+
Seizure	–	–	–	–	–	–	–	–	+	+
EEG	Spike and slow	*NP*	Normal	*NP*	Normal	Normal	Normal	Normal	Spike	Abnormal
MRI[a]	CE, ME, PO	CE, ME, PO	CE, ME, PO	CE, ME, PO	CE, ME, PO	CE, ME[b], PO[b]	CE, ME, PO	CE, ME, PO	CE, ME, PO	CE, ME, PO
Other abnormalities	Bilateral sensory deafness	Craniofacial dysmorphisms, bilateral hydronephrosis, deafness					Bilateral sensory deafness		Severe scoliosis	
Karyotype	46,XX	46,XX	46,XX	46,XX, inv (9)(p12q13)[c]	46,XX	46,XX	46,XX	46,XX	46,XX	46,XX
X-tiling array	NP	NP	–	NP	–	–	del(X) (p11.3p11.4)dn	del(X) (p11.3p11.4)dn	dup(X)(p11.4)	dup(X) (p11.4), dup(X) (p11.21)
Size of CNV (Mb)							3.0	1.1	0.2	Two times 0.2

Table 1 continued

Patient	1	2	3	4	5	6	7	8	9	10
CASK mutation										
Exon	2	4	27	3	Intron 4	Intron 21	None	NP	NP	NP
Nucleotide change	c.79C>T	c.316C>T	c.2632C>T	c.243_244delTA	c.357-1G > A	c.2040-1G > C				
Protein change	*p.R27X*	*p.R106X*	*p.Q878X*	*p.Y81X*	*p.S119Rfs7X*	*p.W680Cfs29X*				
					p.H120Pfs22X	*p.W680Cfs3X*				
CASK aberration in parents	NP	None	None	NP	None	None	None	None	NP	None

NA not available, *NP* not performed, *SD* standard deviation

+, present; –, absent

[a] Showing hypoplastic region: *CE* cerebellum, *ME* mesencephalon, *PO* pons

[b] The hypoplasia is mild

[c] Normal variation

using genomic DNA of patient 10, four unaffected females and one unaffected male using the 7500 Real-Time PCR System (Applied Biosystems) and KAPA SYBR® FAST qPCR Master Mix (KAPA Biosystems) according to the manufacturers' instructions. Primers were designed using Primer3 software. Four primer combinations, Primer 1–4, were designed for the duplication at Xp11.4 between A_16_P21451772 and A_16_P21451795, which were oligonucleotides on the nucleotide array. Six primer combinations, primer 5–10, were designed for the duplication at Xp11.21 between A_16_P03708491 and A_14_P101900. The sequences of the primer combinations are provided in Supplementary Table 2.

Results

Mutation analysis

The analysis detected the mutations probably responsible for the phenotypes in six cases (Table 1; Fig. 2). Nonsense mutations were detected in three cases: c.79C>T (*p.R27X*), c.316C>T (*p.R106X*) and c.2632C>T (*p.Q878X*) in patients 1, 2 and 3, respectively. A deletion of two nucleotides in exon 3 was detected in patient 4: c.243_244delTA (*p.Y81X*). Mutations in intron were detected in two cases: c.357-1G>A of intron 4 in patient 5 and c.2040-1G>C of intron 21 in patient 6. Both intronic mutations were located at the splice acceptor sites and possibly affected the splicing of *CASK*. None of the mutations has been reported previously (Najm et al. 2008; Tarpey et al. 2009). In patients 2, 3, 5 and 6, we did not detect the mutation in either of the parents (data not shown), suggesting the mutations to be de novo.

aCGH analysis and FISH

In four patients without possible causative mutations in *CASK*, CNVs involving *CASK* were detected by aCGH (Table 1; Fig. 3a). Heterozygous deletions including the gene were detected in patients 7 and 8. Duplications were detected in two patients: a 0.2-Mb intragenic duplication within *CASK* was detected in patient 9, and two 0.2-Mb duplications were detected at Xp11.4 within *CASK* and at Xp11.21, including part of *AX747041*, the function of which was unclear, in patient 10. All the CNVs were confirmed by FISH (Fig. 3b). Notably, FISH demonstrated that the duplication was a tandem duplication in patient 9, and that the two duplications in patient 10 were caused by a paracentric inversion between Xp11.4 and Xp11.21. In patients 7, 8 and 10, FISH detected the same CNV in neither of the parents, suggesting the CNVs to be de novo (data not shown). Parental samples of patient 9 were not

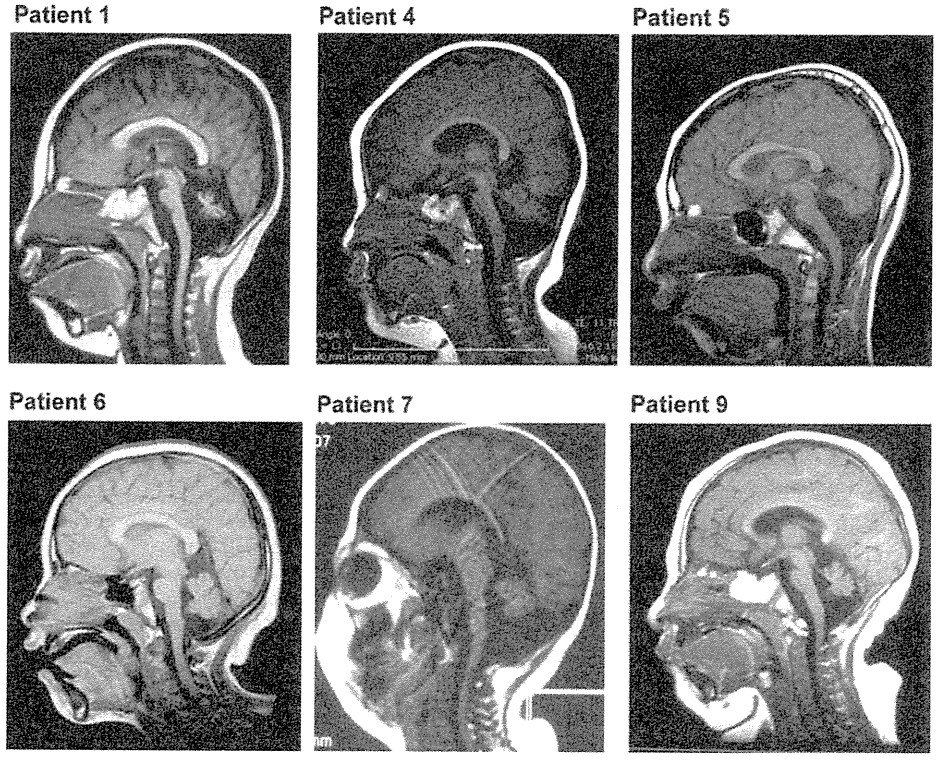

Fig. 1 Representative brain MRI scans in six patients. All of them showed a hypoplastic cerebellum, mesencephalon and pons

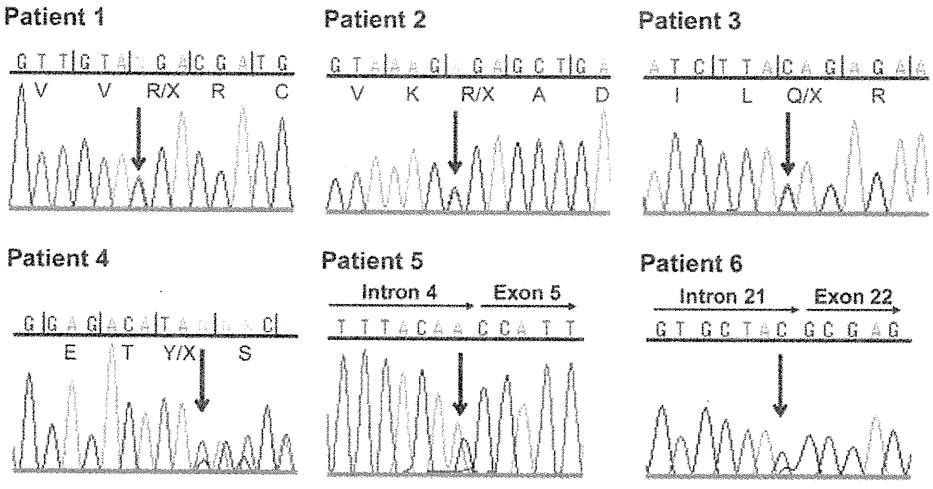

Fig. 2 Partial electropherograms depicting the CASK mutations; c.79C>T in patient 1, c.316C>T in patient 2, c.2632C>T in patient 3, c.243_244delTA in patient 4, c.357-1G > A in patient 5 and c.2040-1G > C in patient 6. Each *arrow* indicates the mutated nucleotide. The translated amino acid sequences are shown under the nucleotides. The *black vertical lines* indicate reading frames

available. A scheme of the deletions and duplications is shown in Fig. 3c.

Transcript analysis

Subsequently, we estimated the effect of the mutations at the splicing acceptor sites. For patient 5, we performed RT-PCR using primer combinations designed to target the area between exon 3 and exon 8 and obtained two products; one was the same size as the wild-type amplicon and the other was a smaller product (Fig. 4a; Supplemental Table 1). The smaller product was cloned and sequenced to show three different-sized transcripts (clone 1–3, Fig. 4b). Clone 1 was a transcript missing all of exon 5 (Fig. 4c) and clone 3 was a transcript in which exon 5 was absent and alternatively a part of intron 5 was inserted (Fig. 4d). Both were aberrant *CASK* transcripts leading to a frameshift and a premature stop codon, *p.S119Rfs7X and p.H120Pfs22X*,

respectively (Table 2). Clone 2 was a normal transcript. For patient 6, we also performed RT-PCR using primer combinations designed between exon 19 and exon 27 to obtain a smaller product than the control (Fig. 5a; Supplemental Table 1). The product was cloned and sequenced to show transcripts of three different sizes (clone 1–3, Fig. 5b). Clone 1 was a transcript without the initial 8 bp of exon 22 (Fig. 5c) and clone 3 was a transcript missing all of exon 22 (Fig. 5d). Both were aberrant *CASK* transcripts leading to a frameshift and a premature stop codon, *p.W680Cfs29X* and *p.W680Cfs3X*, respectively (Table 2). Clone 2 was a normal transcript; therefore, both of the mutations at the splicing acceptor sites caused *CASK* null mutations.

We also estimated the effects of the duplication of *CASK* in patients 9 and 10. Since the results of FISH suggested that an interstitial part of *CASK* was duplicated in patient 9 (Fig. 3b), we precisely mapped the duplication using the oligonucleotide array (Fig. 6a). We predicted the structure of the intragenic duplication and performed RT-PCR using primer combinations designed between exon 7 and exon 4, that is, specific to the duplication, and obtained a product (Fig. 6; Supplementary Fig. 1a; Supplementary Table 1). Sequencing showed the product of the RT-PCR to consist of exon 7 followed by exon 3 (Fig. 6c). These results indicated that the duplication in patient 9 probably caused an aberrant *CASK* transcript leading to a frameshift and a premature stop codon.

In patient 10, FISH suggested that the duplications were a result of a paracentric inversion (Fig. 3b). We also determined the precise size of each duplication with an oligonucleotide array (Fig. 7a) and qPCR (Supplementary Fig. 1b) and predicted a rearrangement in which exon 1, exon 2 and the duplicated exons 3–9 of *CASK* were at Xp11.21. (Fig. 7b). Inversion-specific genomic PCR using a primer combination between intron 8 of *CASK* and intron 1 of *AX747041* supported such a rearrangement (Fig. 7c; Supplementary Table 1). They were potentially transcribed to produce an aberrant transcript with exon 2 of *AX747041* which was originally located at Xp11.21 (Fig. 7b); thus, an inversion-specific RT-PCR using primer combinations targeting between exon 7 of *CASK* and exon 2 of *AX747041* was performed and a product was generated only in patient 10 (Fig. 7d; Supplementary Table 1). Sequencing of this product demonstrated that following exon 9 of *CASK*, exon 2 of *AX747041* was transcribed to produce a stop codon (Fig. 7e). These results clearly proved that the inverted duplication in patient 10 also resulted in *CASK* null mutations.

Fig. 3 Array-CGH analysis and FISH. **a** Results of the X-array analyses. Clones are ordered according to the UCSC mapping position. Each *spot* represents the test/reference value after normalization and $\log_2$ transformation in each BAC clone. The *gray* vertical bar indicates the position of a centromere. *Black arrows* indicate each CNV. An approximately 3.0-Mb deletion at Xp11.4p11.3 was detected in patient 7 and an approximately 1.1-Mb deletion at Xp11.4p11.3 was detected in patient 8. In patient 9, an approximately 0.2-Mb duplication at Xp11.4 was detected based on the increased ratios of one BAC clone. In patient 10, two approximately 0.2-Mb duplications were detected at Xp11.4 and at Xp11.21. **b** Representative results of FISH and enlarged X chromosomes in each patient. *Yellow arrows* denote aberrant signal(s). Of the enlarged chromosomes, the *left* one is intact and the right one is affected, and *white* bands indicate the position of the centromere. In patients 7 and 8, FISH using a probe at Xp11.4 (RP11-95C16, *red*) and a reference probe at Xq28 (RP11-119A22, *green*) confirmed each deletion (*yellow arrow*). In patient 9, FISH using a probe at Xp11.4 (RP11-1069J5, *red*) and the same reference probe delineated tandem duplication (*yellow arrow*). In patient 10, both probes at the two duplications, RP11-1069J5 (*red*) and RP11-1106F5 (*green*), were hybridized at the same position (two *yellow arrows* in the *left enlarged panel*). On the right side, a schematic representation is shown. In the *right enlarged panel*, the probe combination located within the two duplications, RP11-95C16 at Xp11.4 (*red*) and RP11-179I23 at Xp11.21 (*green*), showed an inverted orientation in the affected chromosome X (two *yellow arrows*, *right*) compared with the intact chromosome X (*left*). On the right, a schematic representation is shown. **c** Scheme of the region around *CASK*, BAC clones, genes, deletions and duplications. *Open double-headed arrows* indicate the deletions and *filled double-headed arrows* indicate the duplications. *Horizontal black bars* indicate BAC clones (RP-11 series). *Thin horizontal arrows* indicate genes and their directions. In concordance with ISCN 2005 (Shaffer and Tommerup 2005), this result was described as follows: patient 7, arr cgh Xp11.4p11.3(RP11-829G10 → RP11-469F12)x1; patient 8, arr cgh Xp11.4p11.3(RP11-1069J5 → RP11-52P6)×1; patient 9, arr cgh Xp11.4(RP11 → 1069J5)x3; and patient 10, arr cgh Xp11.4 (RP11-1069J5)×3,Xp11.21(RP11-54I5 → RP11-1106F5)×3 (color figure online)

Discussion

Among the ten cases with phenotypic criteria, female, MR and MICPCH, we detected genomic aberrations of *CASK* in all cases, nonsense mutations in three cases, a 2 bp-deletion in one case, mutations at the splice acceptor sites in two cases, heterozygous deletions encompassing *CASK* in two cases and intragenic duplications in two cases. Not only the nonsense mutations but also mutations at the splice acceptor sites generated aberrant *CASK* transcripts, leading to a frameshift and a premature stop codon. The intragenic tandem duplication in patient 9 and the intragenic inversion/duplication probably due to inv(X)(p11.4p11.21) in patient 10 also produced an aberrant transcript causing a frameshift, leading to a premature stop codon within *CASK*. We previously reported that the heterozygous deletion containing *CASK* probably reduced the expression of intact *CASK* in a female patient (Hayashi et al. 2008). The current study extends the variety of genomic alterations causing *CASK* null mutations. The incidence of *CASK* mutations and of CNVs involving *CASK* was almost the same, and there was no mutational hot spot in *CASK* according to a previous report (Najm

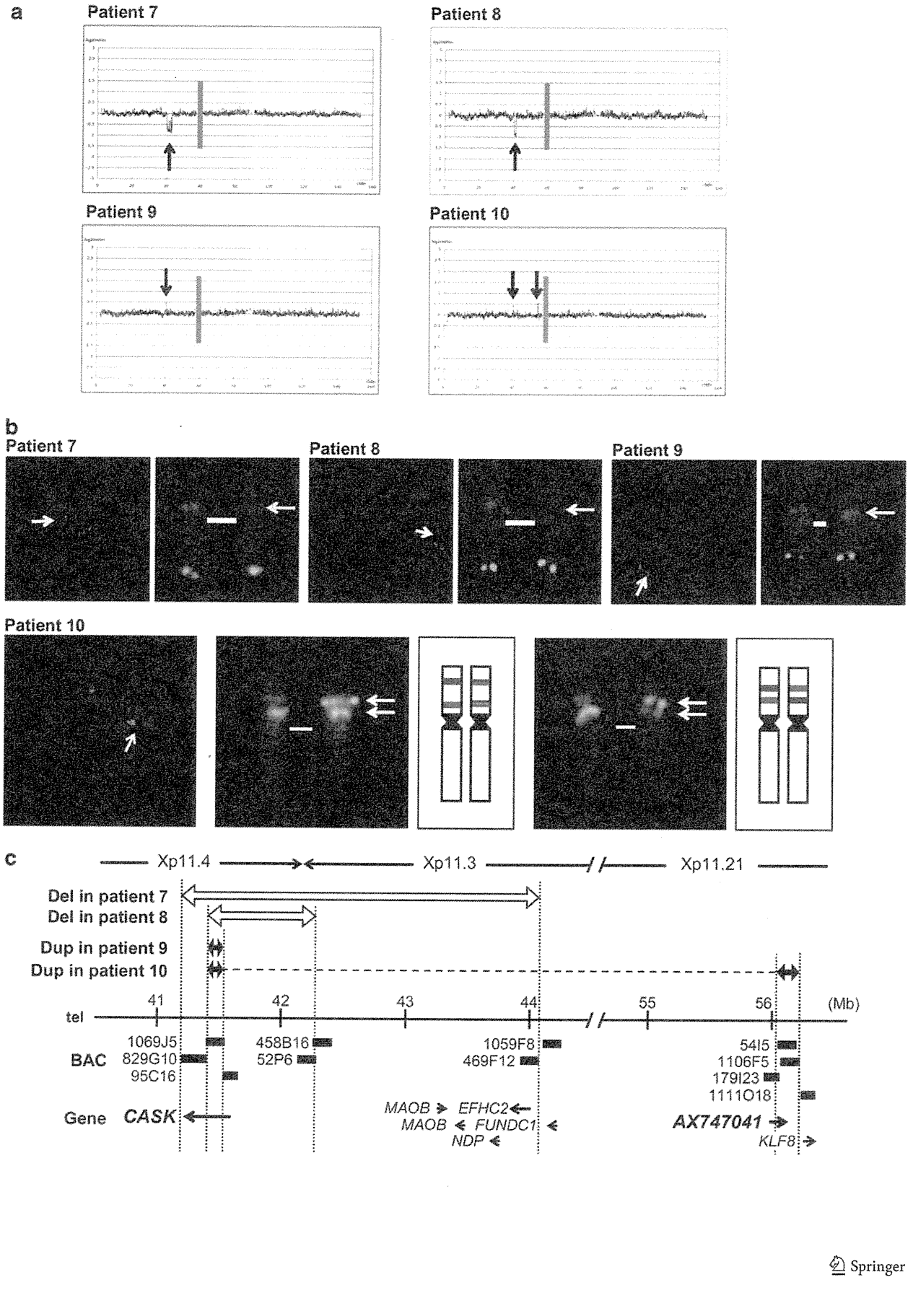
a
Patient 7
Patient 8
Patient 9
Patient 10
b
Patient 7
Patient 8
Patient 9
Patient 10
c
Xp11.4
Xp11.3
Xp11.21
Del in patient 7
Del in patient 8
Dup in patient 9
Dup in patient 10
tel
41
42
43
44
55
56
(Mb)
BAC
1069J5
829G10
95C16
458B16
52P6
1059F8
469F12
54I5
1106F5
179I23
1111O18
Gene
CASK
MAOB
EFHC2
MAOB
FUNDC1
NDP
AX747041
KLF8

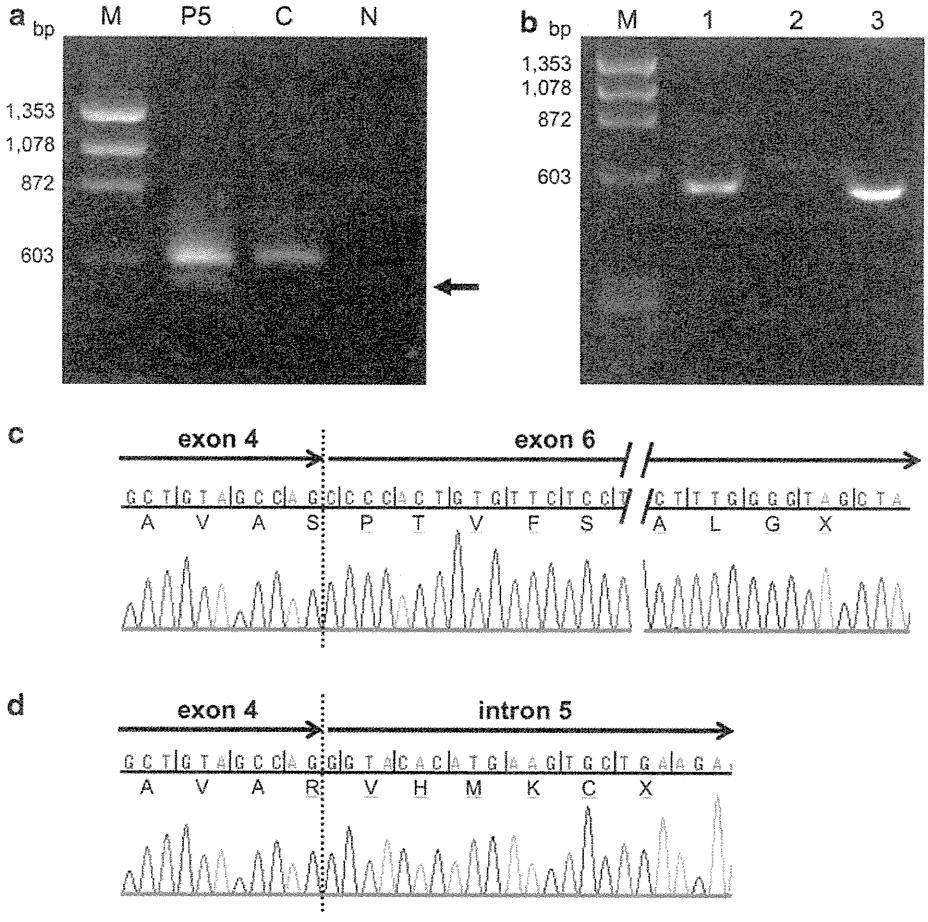

Fig. 4 Exon skipping and aberrant transcripts in patient 5. **a** RT-PCR using primer combinations for exons 3 and 8. The *arrow* indicates an aberrant-sized product in patient 5. *M* marker; ϕX174 RF DNA/Hae III Fragments, *P5* patient 5, *C* control, *N* negative control, no DNA added. **b** The PCR products were cloned to reveal clones of three sizes. Representative clones are shown. No. 1 and no. 3 are aberrant-sized clones and no. 2 is a normal-sized clone. **c**, **d** Sequence chromatograms from clones 1 and 3. In clone 1, exon 5 was skipped to cause an aberrant transcript leading to a frameshift and a premature stop codon in exon 6 (**c**). In clone 3, next to exon 4, exons 5 and 6 were skipped and part of intron 5 was inserted to cause an aberrant transcript leading to a frameshift and a premature stop codon in intron 5 (**d**). The translated amino acid sequences are shown under the nucleotides and *underlines* indicate the frameshift mutations. The *black vertical lines* indicate reading frames. *Dashed vertical lines* denote exon–exon or exon–intron boundaries

et al. 2008) and ours. The molecular mechanism causing the recurrent CNVs remains unclear. For example, known low-copy repeats (LCRs), important factors facilitating nonallelic homologous recombination (NAHR) (Stankiewicz and Lupski 2002), do not adequately explain the CNVs, since no LCRs on/around breakpoints involved in CNVs in any of the current four cases and our previous case (Hayashi et al. 2008) have been registered, even in up-to-date genome databases (UCSC March 2006 and February 2009 build). While the CNVs may be incidental, detailed analyses of the DNA sequence flanking the breakpoints of the CNVs may reveal the mechanisms behind the genomic rearrangement around *CASK* (Inoue et al. 2002).

Recently, *CASK* aberrations have been reported in patients with MR with/without MICPCH (Hsueh 2009) (Table 2). As previously mentioned, a heterozygous nonsense mutation and a disruption caused by a chromosomal inversion were detected in females with severe MR and MICPCH (Najm et al. 2008). They also reported a synonymous mutation causing exon 9 to be skipped in a male, who died at 2 weeks of age. On the other hand, through mutational screening of X-linked MR, four missense mutations of *CASK* were found in male patients with MR (Tarpey et al. 2009). Their MR was mild and two also revealed nystagmus. Moreover, a missense mutation of *CASK* was identified in a family with FG syndrome (Piluso et al., 2009). These reports suggest that *CASK* aberrations cause three very different phenotypes: severe MR with MICPCH in females, mild MR in males and FG syndrome in males, depending on the type of aberration. As *Cask* knockout (KO) mice were reported to die in the neonatal period (Laverty and Wilson 1998; Atasoy et al. 2007), a complete lack of *CASK* is probably lethal, consistent with the male patient with the *CASK* mutation (Najm et al. 2008); however, missense mutations in male patients probably cause different clinical conditions, i.e., mild MR or FG syndrome (Tarpey et al. 2009; Piluso et al. 2009), and haploinsufficiency of

Table 2 Summary of mutations affecting single or few base pairs in the CASK gene

Gender	Phenotype	Type of mutation	Nucleotide change	Protein change	Comment	Report
F	MR/MICPCH	Nonsense	c.1915C>T	*p.R639X*		Najm et al. 2008
M	MR/MICPCH	Synonymous	c.915G > A	*p.=*	Skipping of exon 9 observed; the patient died at 2 weeks	Najm et al. 2008
F	MR/MICPCH	Nonsense	c.79C>T	*p.R27X*		Our case (patient 1)
F	MR/MICPCH	nonsense	c.316C>T	*p.R106X*		Our case (patient 2)
F	MR/MICPCH	Nonsense	c.2632C>T	*p.Q878X*		Our case (patient 3)
F	MR/MICPCH	ins/del	c.243_244delTA	*p.Y81X*		Our case (patient 4)
F	MR/MICPCH	Splice-site mutation	c.357-1G>A	*p.S119Rfs7X* *p.H120Pfs22X*	Skipping of exon 5, or skipping of exon 5 and insertion of partial intron 5	Our case (patient 5)
F	MR/MICPCH	Splice-site mutation	c.2040-1G>C	*p.W680Cfs29X* *p.W680Cfs3X*	Skipping of partial or entire exon 22	Our case (patient 6)
M	FG syndrome	Missense	c.83G>T	*p.R28L*	Skipping of exon 2 observed with low frequency	Piluso et al. 2009
M	Mild MR	Missense	c.2129A>G	*p.D710G*		Tarpey et al. 2009
M	Mild MR	Missense	c.802T>C	*p.Y268H*		Tarpey et al. 2009
M	Mild MR	Missense	c.2767C>T	*p.W914R*		Tarpey et al. 2009
M	Mild MR	Missense	c.1186C>T	*p.P396S*		Tarpey et al. 2009

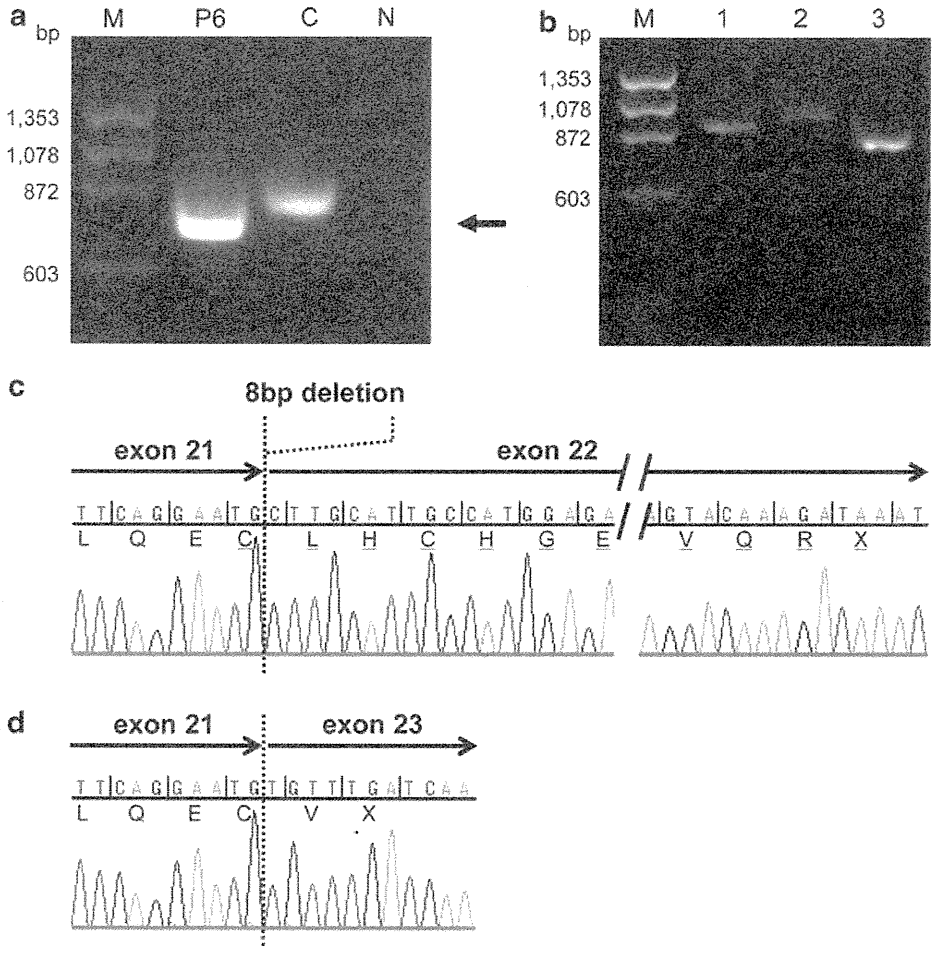

Fig. 5 Exon skipping and aberrant transcripts in patient 6. **a** RT-PCR using primer combinations for exons 19 and 27. The *arrow* indicates an aberrant-sized product in patient 6. *M* marker, ϕX174 RF DNA/Hae III Fragments, *P6* patient 6, *C* control, *N* negative control. **b** The PCR products were cloned to reveal clones of three sizes. Representative clones are shown. No. 1 and 3 are aberrant-sized clones and no. 2 is a normal clone. **c, d.** Sequence chromatograms from clone 1 and 3. In clone 1, the initial 8 bp of exon 22 was absent, causing an aberrant transcript leading to a frameshift and a premature stop codon (**c**). In clone 3, all of exon 22 was missing, resulting in an aberrant transcript leading to a frameshift and a premature stop codon in exon 23 (**d**). The translated amino acid sequences are shown under the nucleotides and *underlines* indicate the frameshift mutations. The *black vertical lines* indicate reading frames. Dashed vertical lines denote exon–exon boundaries

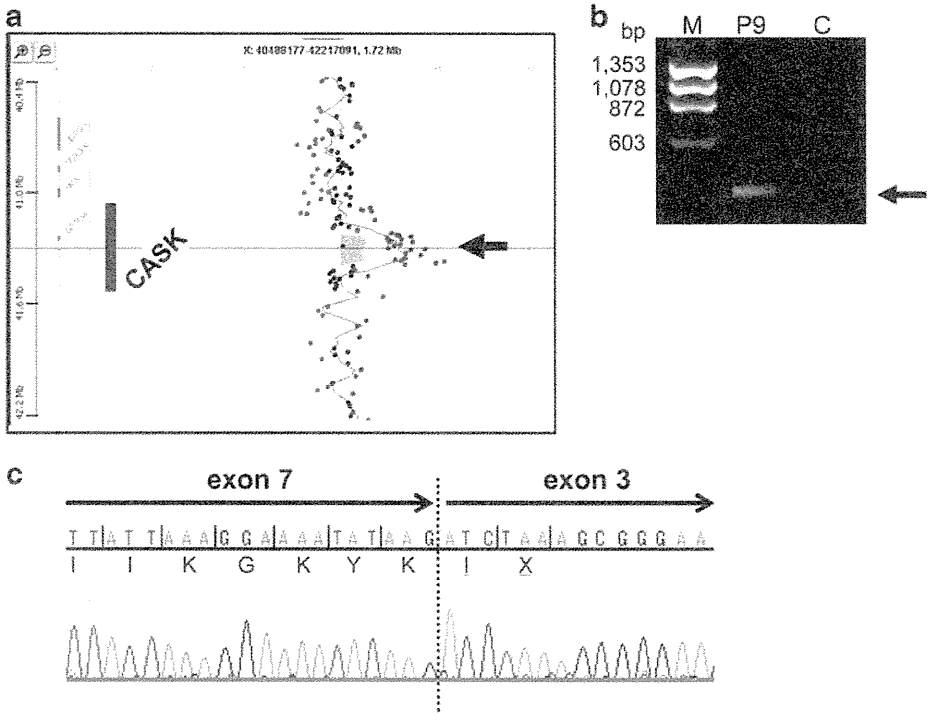

Fig. 6 Analsyses of the duplication in patient 9. **a** Results obtained with Agilent Human Genome CGH microarray kit 244K. This result was described as follows: arr Xp11.4(41,280,790-41,439,415)×3. The duplication included exon 3–7 of *CASK*. It was unclear whether exon 8 was included (*arrow*). The relevant genes are emphasized. **b.** RT-PCR using primer combinations for exon 7 and 4. A product was gained only from patient 9 (*arrow*). *M* marker; ϕX174 RF DNA/Hae III Fragments, *P9* patient 9, *C* control. **c.** Chromatograms for the RT-PCR product shown in (**b**). Next to exon 7, the duplicated exon 3 was transcribed to cause an aberrant transcript leading to a frameshift and a premature stop codon. The translated amino acid sequences are shown under the nucleotides and *underlines* indicate the frameshift mutations. The *black vertical lines* indicate reading frames. *Dashed vertical lines* denote exon–exon boundaries

CASK in females probably causes severe MR with MICPCH (Hayashi et al. 2008; Najm et al. 2008).

CASK encodes a multi-domain scaffolding protein with several critical roles in brain development and synaptic functions, including synaptic interaction, neurotransmitter release and dendritic spine formation (Hata et al. 1996; Irie et al. 1997; Cohen et al. 1998; Hsueh et al. 2000; Olsen et al. 2005; Hsueh 2006; Chao et al. 2008). CASK also regulates the expression of *RELN* involved in brain development through interactions with Tbr-1 via a guanylate kinase (GK)-like domain (Hsueh et al. 2000), and this function may be essential for the etiology of MR with MICPCH. *RELN* plays an important role in neural migration and brain development (D'Arcangelo et al. 1995; Ogawa et al. 1995; Rice et al. 1998), and its mutation is associated with lissencephaly with cerebellar hypoplasia (Hong et al. 2000). While the current analysis provides novel mutations and several types of genomic aberrations of *CASK* causing MR with MICPCH, except for the heterozygous deletions all the mutations and duplications produced aberrant transcripts which will be degraded due to nonsense-mediated mRNA decay and no CASK proteins will be expressed from the mutant alleles; that is, they cause *CASK* null mutations. This may explain the similarity of the phenotypes of MR with MICPCH regardless of the type of *CASK* aberration. The relation between genotypic variety and phenotypic similarity could be clinically useful for detecting and investigating potential patients with *CASK* aberrations.

Web Resources. URLs of the Web sites referred to in this manuscript are as follows:UCSC Genome Bowser, http://genome.ucsc.edu/ (March 2006 build)NCBI, http://www.ncbi.nlm.nih.gov/Online Mendelian Inheritance in Man (OMIM), http://www.ncbi.nlm.nih.gov/Omim/Primer3, http://frodo.wi.mit.edu/primer3/.

Accession Numbers. The *CASK* genomic region is from The UCSC March 2006 build (NCBI36/hg18), range = chrX:41259133-41667231. The GenBank accession number of the human CASK cDNA transcript variant 1 (isoform 1)

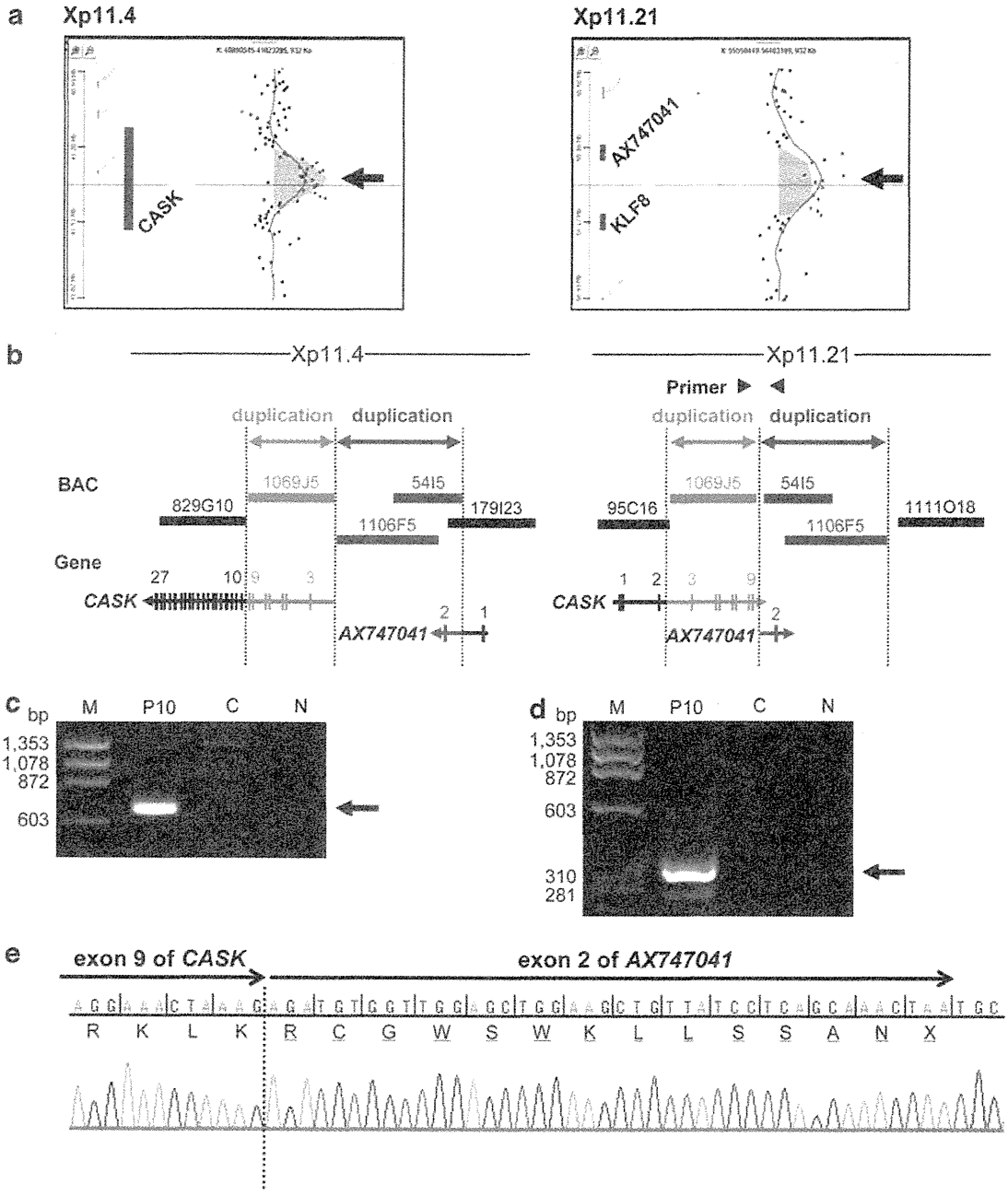

Fig. 7 Analyses of the duplications in patient 10. **a** Results obtained with Agilent Human Genome CGH microarray kit 244K. This result was described as follows: arr Xp11.4(41,381,483-41,539,961)×3, arr Xp11.21(56,022,198-56,272,783)×3. The duplication at Xp11.4 included exons 3–8 of *CASK* (*arrow*, *left panel*) and the duplication at Xp11.21 included exon 2 of *AX747041* (*arrow*, *right panel*). The relevant genes are *emphasized*. **b** A predicted structure of two duplications in patient 10 based on the results of FISH, oligonucleotide array and qPCR. The region denoted by *gray double-headed arrows*, originally at Xp11.4 and including exons 3–9 of *CASK*, was inverted and duplicated at Xp11.21. The region denoted by *red double-headed arrows*, originally at Xp11.21 and including exon 2 of *AX747041*, was inverted and duplicated at Xp11.4. Exons 1 and 2 of CASK and exon 1 of *AX747041* are also involved in the inversion but not duplicated. *Vertical lines* denote exons and *arrows indicate* the direction of *CASK* and *AX747041*, respectively. *Numbers* above the genes denote exons. *Horizontal thick bars* indicate BAC clones (RP-11 series). A pair of *black triangles* indicates the primer combinations for inversion-specific genomic PCR. **c** Inversion-specific PCR revealed a product only in patient 10 (*arrow*). *M* marker; ϕX174 RF DNA/Hae III Fragments, *P10* patient 10, *C* control, *N* negative control. **d** Inversion-specific RT-PCR also revealed a product only in patient 10 (*arrow*). *M* marker; ϕX174 RF DNA/Hae III Fragments, *P10* patient 10, *C* control, *N* negative control. **e** Sequence chromatograms from the RT-PCR product shown in (**d**). Next to exon 9 of *CASK*, exon 2 of *AX747041* was transcribed to cause an aberrant transcript leading to a frameshift and a premature stop codon. The translated amino acid sequences are shown under the nucleotides and *underlines* indicate the frameshift mutations. The *black vertical lines* indicate reading frames. *Dashed vertical lines* denote exon–exon boundaries (color figure online)